Publications of the Astronomical Society of the Pacific
105: 367–373, 1993 April

Rosemary Hill Observatory Lunar Occultation Summary for 1983–1984

GLENN SCHNEIDER AND CHRIS ANDERSON

Astronomy Programs, Computer Sciences Corporation, 3700 San Martin Drive, Baltimore, Maryland 21218
Electronic mail: gschneider@stsci.edu, anderson@stsci.edu

Received 1992 October 2; accepted 1993 January 28

ABSTRACT. The results from photometric observations of 21 previously unreported occultation disappearances obtained during the period 1983 March 24 through 1984 March 12 with the University of Florida's Rosemary Hill Observatory 76-cm reflecting telescope are presented. Statistically significant determinations of stellar diameters are indicated for two stars: 32 Librae (12.2 mas) and BD +22° 1032 (5.45 mas). Diameter measurements of marginal statistical significance are noted for two other stars (9 Cancri and 37 Capricorni). New duplicity determinations are reported for five stellar systems in this sample.

1. INTRODUCTION

A systematic program of the observation and analysis of lunar occultation disappearance events was undertaken at Rosemary Hill Observatory (RHO, latitude = +29° 23′ 59.″4, longitude = 82° 35′ 11.″0W, altitude = 44 m) from 1979 through 1985. The astrometric objectives of this program were threefold. The primary objective was to obtain angular diameter measurements for a variety of stars which had not been previously measured, or to obtain independent measurements of the diameters of stars which had been determined earlier by other observational techniques. The secondary goal was to detect previously unsuspected incidence of stellar duplicity or multiplicity, and by resolving those systems, to determine the characteristics of their individual stellar components. The last objective was to precisely measure the times of geometrical occultation for all observations. The astrometric results from this program were reported to the International Lunar Occultation Centre. For a variety of reasons the results obtained from a number of these observations have not been previously reported. Some of those results are summarized and discussed here.

2. INSTRUMENTATION

All photometric lunar occultation observations in this sample were made at the $f/16$ Cassegrain focus of the RHO 76-cm reflecting telescope. A modified Astromechanics dual-channel photometer, employing dry-ice cooled blue-sensitive 6256S and red-sensitive 9684 photomultiplier tubes, was used for all observations. This set of observations was made in a single color only, using the channel appropriate for the spectral energy distribution on the particular star. In most cases, a Johnson-V filter was used to define the spectral bandpass. Exceptions for specific observations are noted in the discussions of individual events which follow. The diameter of the photometer field was chosen at the time of the observation from a selectable diaphragm wheel to optimize the S/N ratio of each of the events based upon the sky brightness and seeing conditions.

The photometer outputs were coupled with short, low-capacitance signal leads to a fast two-stage DC electrometer amplifier, a modification of a design described by Oliver (1976). The resulting amplified signals were sampled and recorded by the Lunar Occultation Data Acquisition System described by Schneider (1985). Except for the observations of BD +24° 0854 and BD +25° 1364 (Nos. 17 and 21 in this report), a digital sampling rate of 1 kHz was employed. Each 1-kHz sample consisted of two pair-averaged points (measured every 0.5 ms) digitized to 12 bit precision using Analog Devices AD574 Analog-to-Digital converters, and stored in a 4-s circulating buffer. Absolute time reference was achieved by simultaneously sampling and decoding WWVB time signals in another data channel.

3. OBSERVATIONS AND ANALYSES

Photometric observations were obtained for the 21 occultation disappearance events listed in Table 1. Indicated are the predicted topocentric local circumstances for those events and their associated geometrical circumstances, which were provided by Lukac, and used in planning the observations of these events.

To determine the physical quantities of interest (angular diameters of resolvable sources and times of geometrical occultation) a nonlinear least-squares differential-correction (NLLSDC) procedure, based upon the basic technique first described in detail by Nather and McCants (1970), and Nather and Evans (1970), was employed. A number of refinements to this model-fitting technique had been adopted. These included the introduction of probabilistic constraints (Eichhorn 1978), iteratively applying partial parametric adjustments, and dynamically regrouping the residual equation into subsets as suggested by Wilson and Biermann (1976) in an improvement to Wilson and Devinney's (1971) eclipsing binary light-curve code. In the NLLSDC occultation model the latter two of these techniques were constrained based upon the degree of coupling indicated by the covariance matrices of the partial derivatives. The application of these techniques to the occultation model was validated both by Monte Carlo simu-

TABLE 1
Predicted Circumstances of Observed Events

E#	Star	V	SP CL	U.T.	POS	CNT	WATTS	CSP	%I	ELG	AL	L-Dist	P-Vel	A-rate
01	+23 1887	6.3	M3 III	83MAR24 00:55:56	110.4	-11.0	97.4	83S	72	116	78	362038	657.2	0.3756
02	+22 1854	7.2	G0	83MAR24 01:14:46	150.8	-49.6	137.8	43S	72	116	82	360913	336.9	0.2467
03	+23 1042	8.6	M0	83APR18 01:35:12	95.7	-4.3	95.9	83S	25	59	36	368613	843.5	0.4720
04	+22 1032	7.5	K0	83APR18 02:12:03	172.1	-80.3	172.3	7S	25	59	28	369285	153.1	0.0855
05	+21 1939	8.4	K0	83APR21 02:46:31	143.4	-30.0	126.7	53S	58	100	58	364349	661.7	0.3746
06	+20 2244	8.2	F5	83APR21 04:33:56	180.2	-67.4	163.2	16S	59	100	35	366061	347.5	0.1958
07	+17 2156	7.4	K0	83APR22 05:13:38	124.6	-7.0	104.1	77S	70	114	37	366100	809.7	0.4969
08	+05 2587	7.9	K0	83JUN21 02:16:54	63.8	+61.5	40.6	40N	53	93	48	370414	364.9	0.2032
09	-16 4089	5.9	K3 III	83JUN22 03:12:54	111.6	+8.3	98.8	85S	90	143	44	386528	627.7	0.3339
10	-18 6037	6.6	A0	83NOV13 03:35:44	31.0	+28.4	51.8	51N	54	95	20	402184	694.7	0.2563
11	-10 6166	8.7	K0	83NOV15 01:51:29	75.6	-24.5	99.4	78S	72	116	50	397056	574.2	0.2983
12	-00 0139	7.7	K0	83NOV17 00:02:09	99.0	-44.6	121.4	52S	87	138	42	391396	516.3	0.2721
13	-00 0145	8.2	F0	83NOV17 01:20:02	66.1	-15.2	88.5	85S	88	139	55	390238	648.2	0.3426
14	-00 0146	7.7	G5	83NOV17 01:28:05	98.3	-47.6	120.7	53S	88	139	56	390149	449.8	0.2378
15	+00 0159	7.8	K0	83NOV17 03:32:06	104.1	-54.1	126.4	47S	88	139	59	389597	384.9	0.1038
16	-20 6237	5.8	F5	83DEC10 00:06:42	118.3	-58.9	137.9	46S	27	62	31	400741	355.7	0.1831
17	+24 0854	6.9	B8	84MAR11 00:39:30	33.7	+47.3	35.2	36N	53	93	77	374852	385.6	0.2345
18	+24 0868	7.4	K0	84MAR11 01:28:06	125.2	-40.7	126.6	52S	53	93	67	374996	494.1	0.2718
19	+24 0882	8.2	K2	84MAR11 02:15:30	111.1	-23.7	112.4	66S	53	94	57	375321	663.4	0.3481
20	+24 0895	8.9	B9	84MAR11 03:17:08	126.3	-36.1	127.5	51S	54	94	44	375983	618.7	0.3394
21	+25 1364	8.7	K5	84MAR12 03:45:29	61.2	+37.1	56.4	57N	65	107	51	369551	606.3	0.3384

E#	Event Number	CSP	Cusp Angle in Degrees
Star	BD Stellar Catalog Number	%I	Percentage of Lunar Disk Illuminated
V	Apparent V Magnitude of Star	ELG	Elongation from Sun in Degrees
SP CL	Spectral Classification	AL	Altitude Above Horizon in Degrees
U.T.	Predicted Date/Time	L-Dist	Topocentric Distance to Lunar Limb (km)
POS	Position Angle in Degrees	P-Vel	Predicted Topocentric Shadow Velocity (m/sec)
CNT	Contact Angle in Degrees	A-Rate	Angular Closure Rate (Predicted, arcsec/sec)
WATTS	Watt's Angle in Degrees		

lations, and by comparison with independently derived results from other observations as suggested by Ridgway et al. (1980). This NLLSDC computational model, described in detail by Schneider (1985), was in routine use throughout the duration of the RHO occultation program. Following Stecklum (1987), the model was modified to allow for the weighting of the data, in the formation of the mean-square residuals, based on the photon statistics.

Although the stars were treated as spherically symmetric limb darkened disks (using a simple linear limb-darkening law) in every case the limb-darkening coefficients were treated as a fixed input to the model, based upon the stellar spectral types. As noted by Evans et al. (1985), the difference in the strip-brightness distributions between a uniform disk and a fully limb-darkened disk is only 13%. Thus, given the typical noise in a photometric occultation observation and the insensitivity of the angular diameter to variations in limb darkening, the limb-darkening coefficient cannot be found.

4. RESULTS

Table 2 summarizes the principal results obtained from the analyses of the occultation observations. These results fall into four broad categories. Most stars in this sample were found to possess angular diameters which were below the detection limit of about 1 mas imposed by both the observational system and the numerical sensitivity of the NLLSDC code. The angular diameters of such stars are indistinguishable from point sources. Figure 1 is representative of an occultation observation, and the resulting fit, for an unresolved star. The 1984 March 11 occultation disappearance of BD +24° 0854 (SAO 077252, ZC 0835), event No. 17, is shown along with the best fit to the observation found by the NLLSDC process. To illustrate the noise characteristics, and dynamic range of this typical observation, an inset in this figure shows the raw photometric data with the disappearance event approximately centered in a 4-s window.

In two cases stars with unresolved disks were found to be members of "close" occultation binaries. Close (denoted C in the "Duplicity Indicated" column of Table 2) in this context implies that the two members of the system are not sufficiently well separated to allow their occultation diffraction curves to be treated independently. In those cases, a two-star version of the NLLSDC fitting process was employed to simultaneously determine the adjustable systemic parameters. For these double stars Table 2 gives the projected component separations in mas, the magnitude difference (ΔV) between the components, and the 1σ uncertainty in the determination of the V magnitudes of the individual stars using the NLLSDC code (assuming the systemic V magnitudes given in Table 1). Figure 2, showing the occultation of BD +20° 2244 (event No. 6) is typical of the occultation diffraction curves seen for close occultation binaries.

Binary systems with widely separated members result in diffraction curves which are not mutually modulated. In those cases the disappearance of each component is separable and may be treated as a single star by the NLLSDC code. Three such widely separated systems were found in the sample, and are denoted W in the "Duplicity Indicated" column of Table 2. The detection of the secondary components in these three systems was achieved by visual inspection of occultation integral curves (Dunham et al. 1973), such as the one shown in Fig. 3 for BD −00° 0146 (event No. 14). The Universal Times of such secondary occultations were determined by least-squares fitting the linear portions of the integration curves on either side of the secondary events, and determining the intersection of the regression lines.

TABLE 2
Results from NLLSDC and Integral Plots

Event#	U.T.	S/N	DIAMETER	SLOPE	D	A.SEP	ΔV	σV	S/B	Δm0	Δm*
01	00:44:55.877±0.012	9.04	2.70±2.41	-0.5	W	440±~17	~4.1		0.86	4.8	4.6
	00:44:54.731±0.032				"	"	"		"	"	"
02	01:14:46.177±0.004	4.1		+19.3	N				0.62	4.5	4.4
03	01:35:12.172±0.051	3.45		-25.5	N				0.75	4.7	4.5
04	02:12:02.030±0.005	4.22	5.45±2.04	+13.5	N				0.98	5.0	5.0
05	02:46:29.632±0.003	3.95		-3.6	C	6.1±2.7	1.13	±0.14	0.66	4.5	4.4
	02:46:29.594±0.008	"		-16.3	"	"	"	±0.37	"	"	"
06	04:33:58.827±0.007	3.65		-16.1	C	13.2±2.2	0.94	±0.09	0.48	4.2	4.2
	04:33:58.773±0.009	"		-24.3	"	"	"	±0.20	"	"	"
07	05:13:37.199±0.001	5.66		-6.3	N				0.94	4.9	4.0
08	02:16:52.406±0.007	5.11		-1.8	W	32.0±~2	~4.9		0.82	4.8	4.4
	02:16:52.249±0.008	"			"	"	"		"	"	"
09	03:12:53.356±0.007	9.90	12.20±1.86	-10.9	N				0.49	4.2	3.7
10	03:35:43.107±0.018	6.58		-9.2	N				0.67	4.6	4.3
11	01:02:40.701±0.014	2.55		+33.2	N				0.20	3.2	3.2
12	00:02:07.790±0.004	3.14		+28.3	N				0.17	3.0	3.0
13	01:20:01.938±0.011	2.31		-9.8	N				0.11	2.5	2.5
14	01:28:01.981±0.010	3.45		+22.1	W	37.9±2.2	>3.5		0.19	3.6	3.2
	01:28:02.207±0.013	"			"	"	"		"	"	"
15	03:32:06.631±0.005	3.58		-20.8	N				0.20	3.2	3.2
16	00:06:39.731±0.004	5.52	1.74±1.68	+20.3	N				5.52	6.9	6.0
17‡	00:39:28.8 ±0.100	11.88		-3.2	N				2.08	5.8	5.1
18	01:28:05.604±0.005	7.74		-10.4	N				1.35	5.3	4.4
19	02:15:30.366±0.012	3.07		-28.1	N				0.29	3.6	3.6
20	03:17:07.618±0.004	2.69		-20.1	N				0.19	3.2	2.6
21‡	03:35:32.8 ±0.100	2.27		-6.4	N				0.13	2.7	1.9

‡ Sampling rate of 100 Hz was employed for these observations

##	Event Number	D	Duplicity Indicated (W = Wide, C = Close)
U.T.	Time of Geometrical Occultation	A.SEP	Angular Separation in mas (for doubles)
S/N	Star/√[Star + Sky])	ΔV	Magnitude difference between components
DIAMETER	Stellar Diameter (mas)	σV	1σ uncertainty in magnitude determination
SLOPE	Lunar Limb Slope (Degrees)	S/B	Starlight-to-Background Ratio
Δm0, Δm*	Secondary component detection limit estimate (see text)		

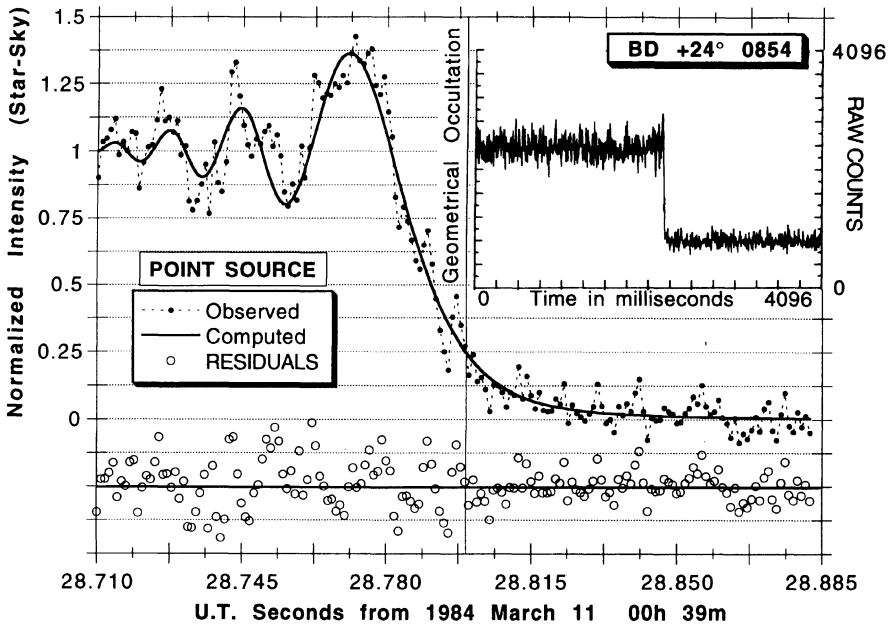

FIG. 1—The NLLSDC fit to the observed diffraction curve for the occultation of BD+24° 0854 was indistinguishable from that of a point source. Residuals, at the same scale, are shown below. The inset at the upper right shows the raw 12-bit photometric data sampled at 1-ms intervals over 4096 ms.

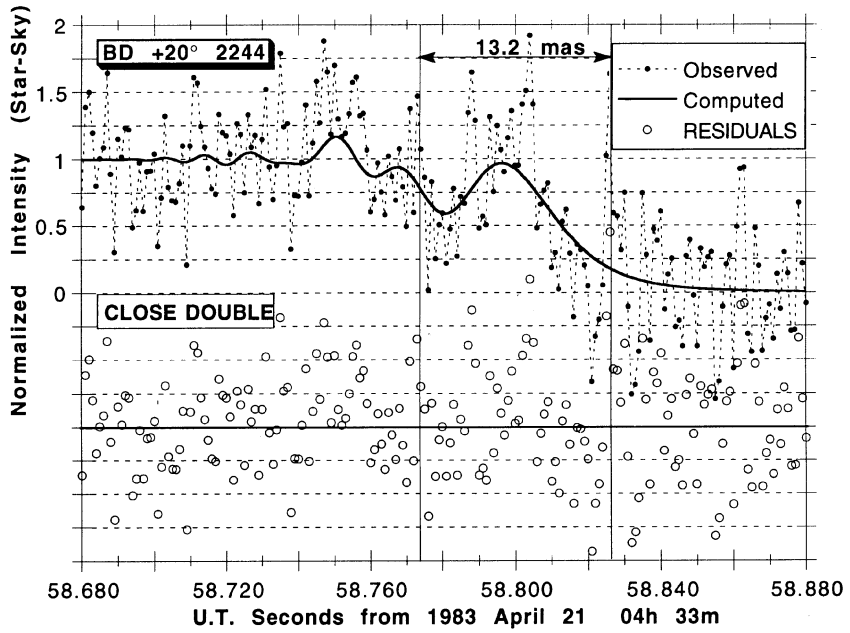

FIG. 2—The two-star NLLSDC solution for the occultation of BD+20° 2244, representative of close occultation binary diffraction curves, found a 13.2 mas projected separation between the stellar components. The vertical lines indicate the times of geometrical occultation for the two components.

For the occultations of 9 Cancri (event No. 1), BD +05° 2587 (event No. 8), and BD −00° 0146 (event No. 14) the newly found secondary components were >3.5 mag fainter than the primary components. Thus, while their existence became apparent, the fringing-related characteristics of the secondary components could not be solved with NLLSDC due to the low S/N ratio for these intrinsically faint components. Table 2 lists the projected angular separation of the components in these systems as determined from their integration curves and the estimated differences in V magnitudes as derived from the change in measured total systemic flux.

In this sample, four stars proved to have sensible angular diameters as noted in Table 2, though two of these (9 Cancri and BD −20° 6237, event Nos. 1 and 16, respectively) were only marginally detectable. Occultation light curves which result from the obscuration of stars with resolvable angular diameters are readily typified by both a reduction in amplitude of the principle diffraction fringe and an accompanying change to the principle fringe width. This, and the associated change (reduction) in the modulation to the higher order fringes, becomes more apparent for stars of larger angular diameters. Figure 4, illustrating the occultation disappearance of 32 Librae (event No. 9) is indicative of an extended source.

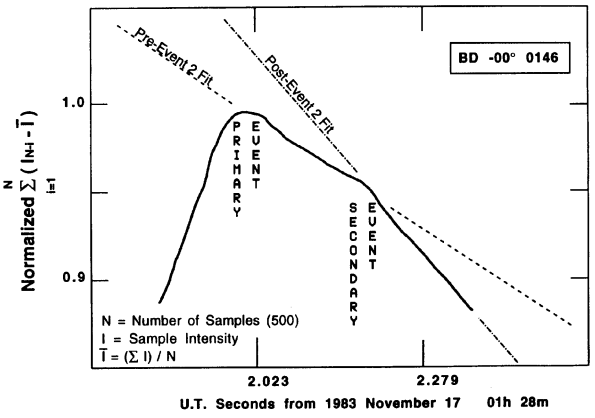

FIG. 3—An occultation integral curve, as discussed by Dunham et al. (1973), for the BD −00° 0146 disappearance event clearly shows two components in this system. The significance of the two linear fits is explained in the text.

For all stars in the sample, the absolute Universal Times of geometrical disappearance, as determined from the NLLSDC procedure, are noted with their error estimates. In this case the timing errors, tabulated in milliseconds, result primarily from difficulties in edge detection of the WWVB signal and do not reflect the much smaller internal errors of the formal NLLSDC solution. For each disappearance, the local slope of the lunar limb at the point of geometrical tangency (the angle of deviation from horizontal, in degrees) is also reported in Table 2. The limb slope, an adjustable parameter fit by the NLLSDC code, enters into the solution as a scale parameter in which the diffraction curve deviates in time from that expected given the predicted angular rate of closure (A rate).

The starlight-to-background ratio (S/B) for each observation is given in Table 2. As described by Radick and Lien (1980), the S/B ratio may be used in determining quantitative estimates of the detectability of a secondary star in the presence of the lunar background alone, and while the primary is unocculted. These estimates, denoted Δm_0 and Δm_* (as per Eitter and Beavers 1974), express the limit of detectability as a minimum magnitude difference between

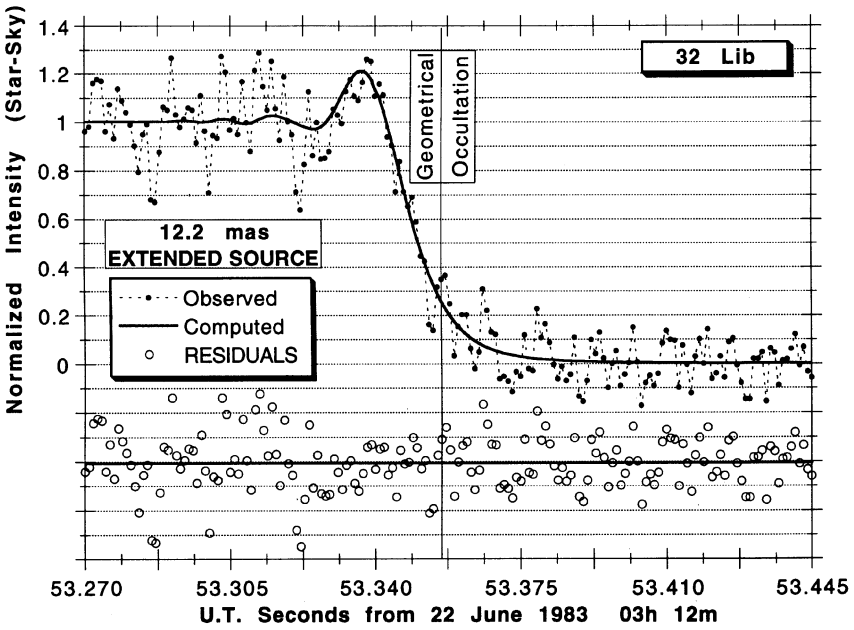

FIG. 4—The occultation diffraction curve from which the unexpectedly large angular diameter of 32 Lib was found is illustrated above. The reduction in fringe visibility and principle fringe width is typical of an extended source.

primary and secondary in these two background regimes. In computing these quantities which appear in the last two columns in Table 2, we have adopted a value of 0.01 as the threshold of detectability (in terms of the S/B ratio) rather than the more conservative value of 0.02 employed by Radick and Lien.

5. INDIVIDUAL EVENTS

Six of the occultations events in this sample (event Nos. 13, 14, 15, 19, 20, and 21) were also observed with the McDonald Observatory 79-cm telescope as reported by Evans et al. (1985). With the exception of an indicated duplicity for RHO event No. 14 (BD −00° 0146, discussed below), their null finding for stellar companions or sensible diameters for these stars is in agreement with ours. BD +00° 0159 (SAO 109577), event No. 15, is a known double (ADS 818AB, GC1185K, X01309) with a distant third companion. However, the $V=8.4$ magnitude secondary component was 25″ from the primary at the time of the occultation and hence well outside of the 7″.5 radius field of view of the photometer.

5.1 Event No. 1—9 Cancri (BD +23° 1887, SAO 079940, ZC 1221)

This bright M3 giant was occulted under favorable conditions on 1983 March 24. A careful examination of an integration plot of this event indicated a slight downward deflection at U.T. 00:44:54.731. This change in the integrated signal level, due to the possible presence of a second star, was rather subtle and was seen more readily in a similar plot centered on the suspected time of the secondary event which excluded the primary disappearance. From a cusp seen in the integration plot at U.T. 00:44:54.711 it was evident that a secondary event did occur. No similar behavior was seen elsewhere in the occultation record when integration plots subsetted over other time regions were plotted. The NLLSDC solution for the time of geometrical occultation of the primary event was found to be 00:44:55.877 U.T. This secondary event occurred 1146 ms earlier. The computed projected velocity of the lunar limb at the point of geometrical contact for the primary event was 691 ± 16 m s^{-1} (corresponding to a local slope of −0.5°), or a radial A rate of 0.3881 arcsec s^{-1}. This implies a projected separation between the two stars of 0.44 arcsec.

The change in mean signal level, due to the fainter star's disappearance (as determined from 500 1-ms samples, both before and after the secondary event) was 0.022 that of the out-of-occultation intensity found for the primary star, or roughly 4 magnitudes fainter. There is, of course, always the possibility of a nonphysically related second star falling coincidentally in the field of view. This observation was made in a circular diaphragm with a 15 arcsec diameter. Thus, the likelihood of such a coincidence is on the order of only one part in 10^7.

Since the secondary event was both faint and well separated in time from the primary (i.e., "wide" in the sense of an occultation binary), the disappearance of the fainter star did not enter into the solution of the primary event. The NLLSDC solution for this event yielded a sensible angular diameter for this star of 2.70 ± 2.41 mas. While the formal error estimate is rather large, a non-point-like solution was indicated. It is noted that the distance of 9 Cancri, derived from its parallax (Hoffleit 1982) is roughly 250 parsecs. This is also indicated by an absolute magni-

tude of −0.7, assumed from its spectral type and luminosity class. Based upon typical characteristics of giant stars (Mihalas and Binney 1981), one would expect a physical diameter for an M3-III star to be on the order of 50 solar diameters. At the indicated distance this corresponds to an angular diameter of 1.9 mas. Thus, the observationally determined diameter presented here is in accord with the previously determined stellar characteristics.

5.2 Event No. 4—BD +22° 1032 (SAO 077559, X07598)

The geometry of this near-grazing event led to a predicted A rate of only 0.0855 arcsec s^{-1}. Hence, the time scale of the observed diffraction phenomena for this event was expected to be roughly four times slower than for a typical event with tangential contact at mid-to-low selenographic latitudes. This indeed was the case. The NLLSDC procedure found a local slope of +13.5°, corresponding to a projected shadow velocity of 136.3±4.4 m s^{-1} or a projected A rate of only 76.2±2.5 mas s^{-1}. This allowed for finer temporal sampling of the diffraction curve than for any other event reported in this paper.

An angular diameter of 5.45±2.04 mas was found for this K0 star. Except for an anomalous drop of approximately 8% in the observed signal intensity 120 ms prior to the time of geometrical occultation in seven contiguous 1-ms samples, the overall fit is quite good. The rather large uncertainty in the determined angular diameter (37% of the diameter itself), was a consequence of both the aforementioned local anomaly, and the general noise characteristics of the sky during this event. Nonetheless, the sensible diameter is statistically significant, being 2.7σ from a point source solution.

5.3 Event No. 5—BD +21° 1939 (SAO 080497, X13534)

The occultation of this K0 star resulted in the first of the two detections of close binaries reported in this sample. Though an initial fitting attempt was made, the single-star NLLSDC model proved to be inappropriate, and incompatible with the photometric data obtained for this event. The binary nature of BD +21° 1939 was revealed by reducing the observation with the two-star NLLSDC model. Neither of the two components in this close system had resolvable stellar diameters. The projected spatial separation of the two components was found to be 6.1±2.7 mas based on the intensity-weighted mean of the determined A rates of 359.3±27.4 mas s^{-1}. The fainter of the two stars underwent disappearance first. The brightness ratio of the components was found to be 2.82±1.29:1. Using a systemic apparent V magnitude of 8.40 (as given in the BD catalog) the individual component V magnitudes would be 8.73±0.13 and 9.86±0.37. The corresponding Universal Times of geometrical disappearance for the two individual components are noted in Table 2.

5.4 Event No. 6—BD +20° 2244 (SAO 080527, X13607)

Given the spectral type of this star (F5), a Johnson-B filter was chosen for this observation. As noted in Table 1, however, the selenocentric angle of the contact point was only 16° from the southern lunar cusp. It was anticipated that this small cusp angle, with the past first-quarter moon, could result in the sky at the geometrical point of contact being significantly brighter in B than V. A check on the sky brightness several minutes before the predicted time of the event indicated that a significantly better $(S+N)/N$ would be obtained with a Johnson-V filter, which was used for the observation.

The second of the two close binary systems reported in this sample was discovered from this star. The unexpected binary nature of BD +20° 2244 was readily apparent in the visual inspection of the raw photometric data (see Fig. 2). The two-star NLLSDC model was used to ascertain the characterizing parameters of this system. Given the early spectral type of this star (and its V magnitude of 8.2) a detectable angular diameter was thought to be unlikely. This indeed was the case both for the primary star, and for the secondary as well.

The fainter of the two components was occulted 53.4 ±7.7 ms before the brighter. From the two-star NLLSDC model the projected separation of the individual stellar components was found to be 13.2±2.2 mas, using an intensity-weighted mean of the determined A rates of 242.6 ±21.23 mas s^{-1}. The brightness ratio of the components was found to be 2.38±0.32:1, or $\Delta V=0.94$ (+0.34, −0.26). Assuming an apparent V magnitude of 8.20 (as noted in the SAO catalog), the individual V magnitudes of the component stars would be 8.59±0.09 and 9.25±0.20, respectively.

5.5 Event No. 8—BD +05° 2587 (SAO 119227, X18067)

The photoelectric digital record of this event was obtained by J. P. Oliver and M. England under very favorable photometric seeing conditions. A faint secondary component was found by examining an integration plot of the event. While the mean signal level dropped by only 3.6% as a result of the secondary disappearance (smaller than any other seen in this reported sample), the 1σ uncertainty in the signal level prior to the secondary disappearance was 0.98%. Hence, the probability of this change in signal level being due to the presence of a previously undetected secondary component exceeds 3.6σ.

The secondary disappearance was seen at U.T. 02:16:52.249±0.008 s, 157±2.2 ms before the time of geometrical occultation of the primary event. From the radial A rate of 203.6±5.90 mas s^{-1}, the two components were found to have a projected separation of 32.0±2.0 mas. Due to both the relatively small signal level of the secondary component and its large separation from the primary disappearance in Fresnel space, the primary occultation diffraction curve was unaffected by the disappearance of the secondary star. The NLLSDC solution for this star, however, did not reveal a measurable angular diameter.

5.6 Event No. 9—32 Librae (BD −16° 4089, SAO 159280, ZC 2209)

The photoelectric observation of the occultation of 32 Lib was obtained on 1983 June 22 by Oliver et al. The

NLLSDC solution to the observed occultation diffraction curve for this event is depicted in Fig. 4. An unexpectedly large angular diameter of 12.18 ± 1.86 mas was found for this K3 giant. This spectral type and luminosity classification, as noted by Hoffleit (1982), along with a V magnitude of 5.92 as tabulated in the SAO Catalog, implies a spectroscopic parallax of approximately 115 pc. From these stellar characteristics one would expect the angular diameter of this star to be an order of magnitude smaller than that found from the occultation observation.

Much effort was spent trying to resolve this apparent disparity. The observational data were critically examined in an attempt to uncover any anomalies. The photometric noise distribution function showed no statistically significant deviation from a Gaussian. Though, as is typical, a very small Poisson tail is seen in the residuals, the magnitude of this was inconsequential and did not bias the NLLSDC fitting process. The power spectra of both the preoccultation star-plus-sky light curve and that of the occultation diffraction curve were also examined. The frequency components in the observed diffraction curve dominated significantly over those of the background noise over the entire frequency domain which is important to the determination of stellar diameters. The numerical fitting process was reviewed and no intrusion of any significant "numerical noise" which could influence the solution was found. The regions of sensitivity of the observed diffraction curve to variations in all parameters in the partial derivatives were found to be both well considered and well behaved. As a result, we could find no reason to dismiss this unexpected result. We suggest that this result should be tested by independent verification, perhaps by speckle or long-baseline interoferometric observations to determine this stellar diameter.

5.7 Event No. 14—BD −00° 0146 (SAO 109552, ZC 0126)

While no stellar diameter was determined for the primary occultation for this star, a secondary disappearance 222.6 ± 8.4 ms after the time of geometrical occultation was detected in the integration plot for this event (see Fig. 3). From the local slope of the lunar limb of +22.1°, as determined from the NLLSDC model, the radial A rate was found to be 170.4 ± 7.55 mas s^{-1}. Thus the projected separation for the two wide stellar components was 37.9 ±2.2 mas. While the time of disappearance of the secondary star could be ascertained as noted, the uncertainty in its contribution to the systemic brightness was quite high. This was primarily due to the characteristics of the scintillation noise during the event. While a quantitative measure of the secondary star's brightness is difficult to ascribe for this event, it can be stated that the fainter component was at least 3.5 mag fainter than the brighter component.

It is unfortunate that no secondary event was detected from McDonald Observatory, as the geometry of the system may have been deduced from observations taken at two different geographic sites. The disparity between the negative finding at McDonald and the secondary detection at RHO is not troubling given the very different geometrical circumstances of the events from these two locations. Evans et al. (1985), have indicated that the maximum ΔV detectable for the post-primary disappearance from McDonald was 3.1. We estimate a ΔV for the two components in this system of at least 3.5.

5.8 Event No. 16—37 Capricorni (BD −20° 6237, SAO 190461, ZC 3158)

The brightness of 37 Cap ($V = 5.79$) allowed this event to be observed with an intermediate bandwidth Strömgren-b filter. As can be seen in Table 2, a formal solution for the angular diameter of this star of 1.74 mas was obtained. However, the 1σ uncertainty in the determination of that free parameter in the NLLSDC model was 1.68 mas, nearly equal to the best estimate of the diameter itself. Thus, this result must be viewed with a high degree of caution, as there is a significant probability ($> 1/3$) that this actually was a point source. This large uncertainty was due to the amplitude and temporal characteristics of the background sky noise during this observation.

We would like to thank John P. Oliver, whose assistance throughout the early stages of this investigation was invaluable. We would also like to thank Martin England and Howard Cohen for their assistance in obtaining the observational records of BD +05° 2587 and BD −16° 4089. Our gratitude is also extended to Marie Lukac and the USNO for providing topocentric occultation predictions for RHO. This work was partially supported by a grant from the University of Florida's Division of Sponsored Research.

REFERENCES

Dunham, D. W., Evans, D. S., McGraw, J. T., Sandmann, W. H., and Wells, D. C. 1973, AJ, 78, 482
Eichhorn, H. 1978, MNRAS, 182, 355
Eitter, J. J., and Beavers, W. I. 1974, ApJS, 28, 405
Evans, D. S., Edwards, D. A., Frueh, M., McWilliams, A., and Sandmann, W. H. 1985, AJ, 90, 2360
Hoffleit, Dorrit, 1982, The Bright Star Catalog (New Haven, Yale University)
Lukac, M. 1983, U.S.N.O. Lunar Occultation Predictions for 1983
Lukac, M. 1984, U.S.N.O. Lunar Occultation Predictions for 1984
Mihalas, D., and Binney, J. 1981, Galactic Astronomy Structure and Kinematics (San Francisco, Freeman)
Nather, R. E., and Evans, D. S. 1970, AJ, 75, 575
Nather, R. E., and McCants, M. M. 1970, AJ, 84, 872
Oliver, J. P. 1976, Rev. Sci. Instrum., 47, 581
Radick, R., and Lien, D. 1980, AJ, 1053
Ridgeway, S. T., Jacoby, G. H., Joyce, R. R., and Wells, D. C. 1980, AJ, 85, 1496
Schneider, G. 1985, Ph.D. dissertation, University of Florida
Stecklum, B. 1987, AJ, 94, 201
Wilson, R. E., and Bierman, P. 1976, A&A., 48, 349
Wilson, R. E., and Deviney, E. J. 1971, ApJ, 166, 605